

Acute Leukemia Classification Using Sequential Neural Network Classifier in Clinical Decision Support System

Ivan Vincent[†], Thanh.T.T.P[†], Suk-Hwan Lee^{††} and Ki-Ryong Kwon[†]

[†]Dept. of IT Convergence and Applications Eng., Pukyong National University

^{††}Dept. of Information Security, Tongmyong University

Summary

Leukemia induced death has been listed in the top ten most dangerous mortality basis for human being. Some of the reason is due to slow decision-making process which caused suitable medical treatment cannot be applied on time. Therefore, good clinical decision support for acute leukemia type classification has become a necessity. In this paper, the author proposed a novel approach to perform acute leukemia type classification using sequential neural network classifier. Our experimental result only covers the first classification process which shows an excellent performance in differentiating normal and abnormal cells. Further development is needed to prove the effectiveness of second neural network classifier.

Keywords:

Acute Leukemia Classification, Sequential Neural Network, Clinical Decision Support System

1. Introduction

Leukemia or white blood cancer is considered as one of the most fatal diseases for the human being. It attacks white blood cells, one of human blood components, which responsible for immune system and disease prevention in the human body. According to French-American-British classification, there are four types of leukemia disease which are classified based on their severity level and infected cells type, they are Acute Myeloid Leukemia (AML), Acute Lymphoid Leukemia (ALL), Chronic Myeloid Leukemia (CML), and Chronic Lymphoid Leukemia (CLL). In this paper, we would like to propose a novel approach to perform only acute leukemia type classification utilizing effective classifier architecture. The proposed method includes several conventional image pre-processing, image clustering, and image segmentation method to extract region of interest, along with feature extraction analysis using PCA method, and finally followed by neural network classifier which provide an excellent performance in classification process that reach 97.75% of accuracy to discriminate normal and cancerous cell images from given database.

2. Related Works

2.1 Overview of Leukemia

A. Acute Lymphocytic Leukemia (ALL)

Acute Lymphocytic Leukemia (ALL) is one between two classes of acute leukemia which develop from early (immature) forms of *lymphocytes* cells in bone marrow. ALL is recorded as the most common of the 4 major types among children but the least common types in adults, but most deaths occur in adults which are understandable because children's bodies can often handle aggressive treatment better than adult's. Most leukemia infected white blood cells has average size about two times the red blood cells that surround them, while normal white blood cells have an average size that similar with the surrounding red blood cells. In most of ALL infected cells, the nucleus area occupies almost 80-90% of the whole cell and left about 20-30% of cell area for the cytoplasm. This feature can be considered as the most distinguishable features to identify ALL from AML type, while another key feature to differentiate ALL and chronic type is that so many granules inside the cell which indicates that the surface of ALL cell is smooth.

B. Acute Myeloid Leukemia (AML)

Acute Myeloid Leukemia is developed from early (immature) forms of *myeloid* cells in bone marrow. AML cases generally occur in older people and uncommon before the age of 45. AML cases hold the most number of deaths among the 4 types of leukemia. The nucleus area is about 50-60% of the whole cell area and about 40-50% cell area is cytoplasm. Sometimes short purple stripes which called "Auer rods" can be found in the cytoplasm area and it makes AML identification become easier.

C. Chronic Lymphocytic Leukemia (CLL)

Chronic Lymphocytic Leukemia is a type of leukemia that attacks the lymphocytes, different from ALL which attack the immature form of lymphocytes. CLL cell has a

similar characteristic with ALL with a small area of cytoplasm and almost 80-90% of the cell area is occupied by nucleus area. The difference between ALL and CLL is the existence of nucleoli inside the nucleus area. Because CLL is basically mature cells which development has been completed, there should not be any nucleolus detected inside CLL cells. The existence of nucleolus can be detected by performing curvelet transform on each CLL cells. This feature is considered to be the key feature to differentiate between ALL and CLL.

D. Chronic Myeloid Leukemia (CML)

Chronic Myeloid Leukemia is another type of chronic leukemia that attacks the myeloid cells and has a similar behavior like CLL, especially in the development state. The average age at diagnosis of CML is around 64 years old. CML cell has a similar characteristic with AML in terms of cytoplasm area ratio, CML also show a big portion of cytoplasm in the cell and most of CML cells are fully developed into mature white blood cells which make it as the most differentiable cells among the four leukemia types. CML nucleus has developed into differentiable shape and texture unlike AML which in most cases the shape is round and under developed. These features of CML could be the key features to differentiate CML from the other types of leukemia cells.

3. Proposed Classification Methodology

3.1 Framework and Constraints

Because we can roughly classify normal and abnormal white blood cell images based on the number of white blood cells exist under one frame of peripheral blood smear image. We proposed a method consist of two main parts, the first part is the pre-classification which mostly about image pre-processing, and the second part is the sequential classification procedure which consists of two neural network classification procedure that constructed by feature extraction and neural network classifier. The full framework of the proposed method describes in Fig. 1.

In this experiment, the full plane blood smear image is used as our experimental objects. We used 100 images in total with 90 training images which processed through this algorithm to obtain trained networks and 10 testing images are preserved as cross-validation images. Since a full plane cell images are used instead of single cell images, this system has a huge potential to be one of the building modules in automatic leukemia decision support system. We extend neural network classifier into further usage by adding the neural network classifier one after another. This classification has an advantage in lower computation cost for each classifier yet could achieve a good classification

performance compare to SVM algorithm in the classification process.

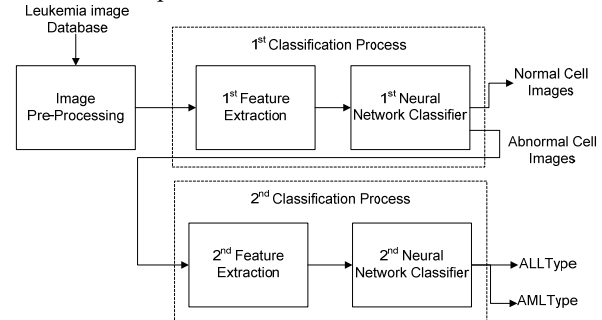


Fig. 1: The main framework of the proposed methodology.

The proposed methodology offers a novel approach to classify leukemia disease along with certain constraints in order to show the best performance. This constraint includes all image in the database need to be normalized into certain magnification and size without any image processing alteration beforehand because our point of interest is to observe the image as a whole image with multiple nucleus inside one image. Each image also should have a standard coloring system in order to preserve the color clustering process in line with the desired classification result.

3.2 Image Pre-processing, Clustering, and Segmentation

3.2.1 RGB to CIE L*a*b Color Conversion

Image pre-processing start with reading the sample image and convert its color space from RGB to CIE L*a*b which consist of luminosity layer L, chromaticity layer a* and layer b* to simplify the process in color based clustering since it reduces the color dimension from 3 dimensions into 2 dimensions. Fig. 2 shows the result of color space transformation and visualization of each layer.

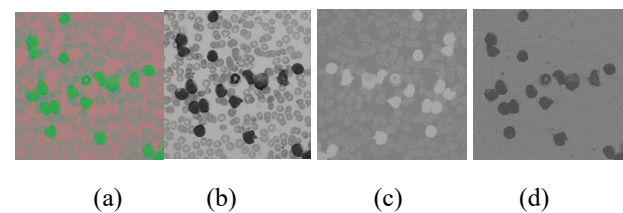


Fig. 2: (a) Result of color space transformation RGB to CIE L*a*b, (b-d) display the luminosity layer L, chromaticity *a layer, and *b layer respectively.

3.2.2 Three Classes K-means Clustering

The resulting image is used in the following k-means clustering which separates the image into 3 different classes based on their color information. Our motivation to separate the image into 3 different classes is inspired from the nature of blood smear image itself which consists of white blood

cells, red blood cells, platelets, and background. Since the white blood cells have a very distinguishable color feature compare to other blood components, the k-means algorithm specifically clusters the white blood cells into its nucleus, cytoplasm, and background as first, second, and third cluster respectively.

3.2.3 Otsu’s Thresholding, Morphological Filter, Area Opening, and Mask Building

For nucleus segmentation process, firstly we choose the nucleus cluster class as our region of interest and apply a sequence of mask building technique start from OTSU auto-thresholding to make a binary image from the first cluster and if the resulting image shows some area others than the region of interest, applying morphological filter such as area opening and closing can help to eliminate those unwanted segmented areas. In this experiment, we use area opening morphological filter with a 1-pixel diameter disk kernel shape and a closing morphological filter with 5-pixel diameter disk kernel shape. These diameter numbers are obtained based on an experiment using the provided image database. The real challenge in nucleus segmentation method lies in determining the diameter value for morphological filter's kernel because it really depends on the image that we use in the experiment. There are 2 results from the previous steps, they are nucleus segmented image and the nucleus segmented mask which will be used in further steps.

3.3 Grouped Cells Separation Procedure

As observed through experiments, it can be seen that in each peripheral blood smear image frame there is a high likelihood for grouped white blood cells appears in the image frame. This thing can cause a problem to the following process, especially shape feature calculations from each cell. Due to this reason, grouped cell separation technique is needed to be performed to ensure that the shape feature calculation is executed for each individual white blood cell.

Watershed algorithm is used in this separation process since it is very suitable to perform segmentation for blood cells which have a circular shape. Watershed algorithm segments each white blood cells into different "catchment basins" based on distance transform which calculate the distance from every pixel to the nearest non-zero-valued pixel. Although it has a very good segmentation performance on almost circular shapes cells, this algorithm still shows some defect in segmenting irregular or random shape objects.

For this experiment, we only used single watershed transform for all sample images to produce “single nucleus mask images” which has the same dimension with the nucleus segmented images.

3.4 Feature Selection and Extraction

3.4.1 Feature Selection and Extraction for Normal and Abnormal Cell Images

For the first classification process, since we only need to differentiate between normal and abnormal cells, such as energy, entropy, contrast, correlation, and Hausdorff dimension value of white blood cells in one frame as shown in Fig. 3. These features can be categorized as textural features which are considered as easy or simple features to detect and show a very good differentiation ability.

Set P_{ij} for an ij^{th} elements of the normalized symmetrical GLCM and N for the number of gray level in the image, the definitions of each feature are elaborated in the following section.

1) Energy measures the homogeneity of an image based on each GLCM value of calculated pixels follows equation (1).

$$Energy = \sum_{i,j=0}^{N-1} (P_{i,j})^2 \quad (1)$$

2) Entropy is a statistical measure of randomness that can be used to characterize the texture of an input image follows equation (2).

$$Entropy = \sum_{i,j=0}^{N-1} -\ln (P_{i,j})P_{i,j} \quad (2)$$

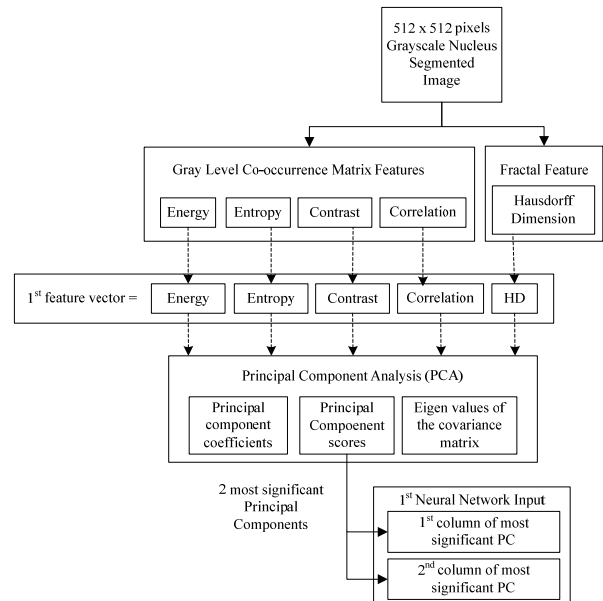


Fig. 3: Feature selection procedure for the first feature vector.

3) Contrast represents a different moment of the regional co-occurrence matrix. It measures the contrast or a number of local variations present in an image follow equation (3).

$$Contrast = \sum_{i,j=0}^{N-1} P_{i,j}(i - j)^2 \quad (3)$$

4) Correlation measures the regional pattern of linear dependencies in the image follows equation (4).

$$\text{Correlation} = \sum_{i,j=0}^{N-1} P_{i,j} \frac{(i-\mu)(j-\mu)}{\sigma^2} \quad (4)$$

μ is the GLCM mean (being an estimate of the intensity of all pixels in the relationships that contributed to the GLCM) and σ^2 is the variance of the intensities of all reference pixels in the relationships that contributed to the GLCM. μ and σ^2 can be calculated follows equation (5) and (6).

$$\mu = \sum_{i,j=0}^{N-1} i(P_{i,j}) \quad (5)$$

$$\sigma^2 = \sum_{i,j=0}^{N-1} P_{i,j} (i-\mu)^2 \quad (6)$$

5) Hausdorff Dimension is one type of fractal dimension which has been widely used in medicine and science research for various quantitative measurement [23, 24]. In this experiment, Hausdorff dimension is used to measure nucleus perimeter roughness and it is considered as an essential feature that can classify normal and abnormal cell images. Hausdorff dimension procedure which is based on box counting method can be calculated by firstly obtain the binary image from grayscale image of the nucleus segmented image and apply edge detection technique to trace out the nucleus boundary. The next step is to superimpose the boundary edges by a grid of squares and count the Hausdorff Dimension using equation (7).

$$HD = \frac{\log(N)}{\log(N(s))} \quad (7)$$

Where (N) is the number of squares in the superimposed grid and ($N(s)$) is the number of occupied square or boxes (box count). Higher HD value implies a higher degree of roughness on the nucleus perimeter.

In this experiment, since all sample images consist of many nucleuses, HD value shows a huge difference between normal and abnormal cells. Thus make Hausdorff Dimension as a very crucial feature in the first classification procedure.

3.4.2 Feature selection and extraction for myeloid and lymphocytic leukemia cell images

For the second classifier which will classify between Acute Lymphocytic and Myeloid Leukemia Type, the classification process needs a more complicated features such as several shape features for each cell blobs. By using these features the difference between ALL and AML can be estimated and distinguish very well.

(1) Cell Area: Each leukemia cells have different characteristic, one of the most obvious features is white blood cell area. By measuring segmented cell area, we can get information about how many pixels are occupied by the actual white blood cells. In this experiment, the counted cell area is the total of all detected cells inside one frame follows equation (8).

$$\text{Cell Area} = \sum_i \sum_j p(i,j) \text{ where } p(i,j) = \begin{cases} 1, & \text{inside cell RoI} \\ 0, & \text{otherwise} \end{cases} \quad (8)$$

(2) Nucleus Area: White blood cell is mainly constructed from a nucleus and surrounded by cytoplasm. Since leukemia type could possibly differentiate based on this features, it is important to acquire nucleus area information from each white blood cell. There is various method to count nucleus area, one of the methods is to count the occupied pixel inside the nucleus Region of Interest (RoI).

$$\text{Nuc Area} = \sum_i \sum_j p(i,j) \text{ where } p(i,j) = \begin{cases} 1, & \text{inside nucleus RoI} \\ 0, & \text{otherwise} \end{cases} \quad (9)$$

(3) Cytoplasm Area: The other important feature to acknowledge leukemic cells is the area of cytoplasm. This feature will be used in ratio calculation between cytoplasm and nucleus area. By successfully calculate cytoplasm area, we could possibly know the difference between AML and ALL. Since cell area and nucleus area has been known beforehand, cytoplasm area can be simply calculated by subtracting nucleus area from cell area.

$$\text{Cyt Area} = \text{Cell Area} - \text{Nuc Area} \quad (10)$$

(4) Nucleus to Cytoplasm Area Ratio (N:C Ratio): This feature will indicate the area ratio between nucleus and cytoplasm. The purpose is to compare the region between nucleus and cytoplasm in all cells. This information is used for type classification since AML has a larger cytoplasm area than ALL it makes ALL has a larger NC ratio than AML. Increase in N:C Ratio commonly indicates the increment in cancerous cells activity.

$$\text{Nuc: Cyt Ratio} = \frac{\text{Nuc Area}}{\text{Cyt Area}} \quad (11)$$

(5) Nucleus to Cell Area Ratio (N: Cell Ratio): This feature will indicate the area ratio between nucleus and the whole cell area. This ratio information is very important as one of the key features for AML and ALL differentiation algorithms since it has been analyzed in the literature that ALL has a larger nucleus to cell area ratio than AML.

$$\text{Nuc: Cell Ratio} = \frac{\text{Nuc Area}}{\text{Cell Area}} \quad (12)$$

3.5 Sequential Neural Network Classifier

3.5.1 Neural network classifier concatenation

Since neural network method is famous for its good accuracy in classification performance after sufficient training, the authors are inspired to experiment on a concatenation of two neural networks not only to obtain a good classification result but also shorten processing time in testing procedure. In order to build sequential neural network classifier architecture, both neural network classifiers should be concatenated in one sequential system. Thus, in this thesis, the concatenation process can be seen at the second classifier where all abnormal cells are processed by the second classifier to classify between AML and ALL leukemia types. The neural network structure that used in this experiment is purposely made as simple as possible to ensure an optimum processing time between each other.

3.5.2 First neural network classifier

First neural network classifier purpose is to classify between normal and abnormal cells. The input of this classifier is the first two columns of the most significant principal components, thus occupy each input node in the classifier. Each hidden node received some load from input load (Xi_k) along with input-to-hidden weight ($Wi_{k,j}$) and hidden node bias (Bi) following equation (13).

$$ni_j = \sum_{k=1}^2 \sum_{j=1}^3 Xi_k \cdot wi_{k,j} + Bi_j \quad (13)$$

The resulted calculation is processed by transfer function ($Fn(ni_{i,j})$) and produce another weight to output layer wo_j and summed with bias from output nodes (Bo) follows equation (14) to produce the output node *value*(no), thus the final output

$$no = \sum_{j=1}^3 Fn(ni_j)wo_j + Bo \quad (14)$$

$$output = \sum_{j=1}^3 \left(\sum_{k=1}^2 Xi_k \cdot wi_{k,j} + Bi_j \right) wo_j + Bo \quad (15)$$

The selected transfer function from the input layer to hidden layer is tangential sigmoid which formula is as shown in equation (16) and Fig. 4(a) shown tangential sigmoid function shape.

$$\tan(sig(x)) = \frac{2}{(1+\exp(-2x))-1} \quad (16)$$

While the transfer function from hidden layer to output layer is the ordinary pure line function or linear transfer

function that follow equation (17) and has a shape as shown in Fig. 4. (b).

$$f(x) = x \quad (17)$$

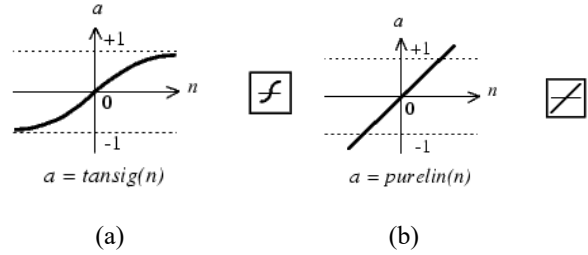


Fig. 4: (a) Tangential sigmoid transfer function and (b) linear transfer function.

The complete neural network classifier architecture can be seen in Fig. 5.

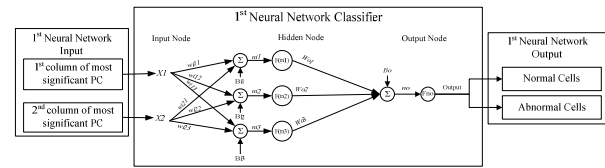


Fig. 5: First Neural Network Classifier Architecture which consists of 2 input nodes, 3 hidden nodes, and 1 output node to classify normal and abnormal cell images.

3.5.3 Second neural network classifier

In the second neural network classifier, instead of classifying normal and abnormal cell images, this classifier focus in classifying between acute lymphocytic leukemia (ALL) and acute myeloid leukemia (AML). However, this classifier uses exactly the same network architecture as the previous classifier as shown in Fig. 6.

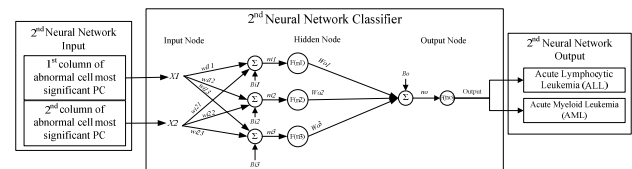


Fig. 6. Second Neural Network Classifier Architecture which consists of 2 input nodes, 3 hidden nodes, and 1 output node to classify ALL and AML cell images.

Both neural networks are trained using Levenberg-Marquardt (LM) algorithm to reach the predetermined target which is gathered from ground truth database information. Levenberg-Marquardt (LM) algorithm is an iterative technique that locates the minimum of a multivariate function that is expressed as the sum of squares of nonlinear real-valued functions. This algorithm has become a standard technique for nonlinear least-squares problem which has been widely adopted in a broad spectrum of disciplines including neural network training scheme.

LM algorithm is actually a combination of two minimization methods, they are gradient descent methods and Gauss-Newton method which will be briefly described as follows. Gradient descent method is a general minimization method which updates parameter values in the direction opposite to the gradient of the objective function. It is recognized as a highly convergent algorithm for finding the minimum of simple objective functions. This method can be modeled by the gradient of the chi-squared objective function with respect to the parameter as shown in equation (18).

$$\frac{\partial}{\partial p} X^2 = (y - \hat{y}(p))^T W \frac{\partial}{\partial p} (y - \hat{y}(p)) = -(y - \hat{y}(p))^T W \left[\frac{\partial \hat{y}(p)}{\partial p} \right] \quad (18)$$

Where $[\partial \hat{y} / \partial p]$ represents the local sensitivity of the function \hat{y} to variation in the parameter p . Thus the derivative (h) that moves the parameters in the direction of steepest descent is shown in equation (19).

$$h_{g,d} = \alpha J^T W (y - \hat{y}) \quad (19)$$

Where α in this equation represents the length of a step in the steepest-descent direction.

Another method that forms LM algorithm is Gauss-Newton method which is also a method for minimizing a sum of – squares objective function. For moderately-sized problems, the Gauss-Newton method typically converges much faster than gradient-descent methods as mentioned in [18]. Gauss-Newton method formula derivation as presented in [18] produce a similar perturbation formula as described in equation (20).

$$[J^T W J] h_{gn} = J^T W (y - \hat{y}) \quad (20)$$

From both mentioned method, LM algorithm adaptively varies the parameter updates between the gradient descent update and the Gauss-Newton update following equation (21)

$$[J^T W J + \lambda I] h_{lm} = J^T W (y - \hat{y}) \quad (21)$$

Where λ is the key parameter in LM algorithm which indicates which update that the algorithm should follow. If the λ value is small the LM algorithm will follow Gauss-Newton update, on the other hand, if the λ value is big then the LM algorithm will follow gradient descent update. The λ value is initialized to be large and gradually getting smaller approaching Gauss-Newton method if the algorithm has approached its solution thus typically converges rapidly to a local minimum. The final update equation from LM algorithm is expressed in equation (22).

$$[J^T W J + \lambda \text{diag}(J^T W J)] h_{lm} = J^T W (y - \hat{y}) \quad (22)$$

Equation (22) is considered as a fundamental expression in this neural network learning algorithm.

4. Experimental result

4.1 Image pre-processing, clustering, and segmentation result

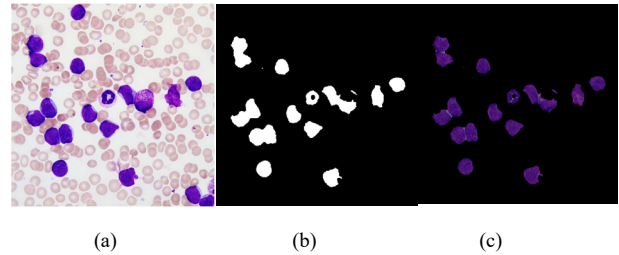


Fig. 7. (a) Original blood smear image, (b) binary mask of segmented region of interest, (c) nucleus segmented image.

Fig. 7 (a) shown an example of 90 images that are used in training procedure. After went through image preprocessing, clustering, and segmentation process as mentioned in section II, binary image mask and nucleus segmented image are produced as depicted in Fig. 7(b) and 7(c) respectively.

Fig. 8(a) shows the first principal component analysis result. As can be seen in the figure, the red circle marks represent abnormal cells while the blue "x" marks represent the normal cells. Between them, there is a green line which estimates the differentiation borderline between abnormal and normal cell images.

4.2 Feature extraction results

Through this visualization, the extracted features could be evaluated as most important or less important features. In this case, the first PCA result consistently states that the extracted features show a quite high importance. Through previous experiments it is known that contrast and Hausdorff's dimension features are the most significant features that can differentiate normal and abnormal cells.

Fig. 8(b) shows the second principal component analysis on the abnormal cell images. The red circle marks indicate ALL cell images while the blue "x" marks indicate AML cell images. This figure clearly shows that the selected features have a high significance since ALL marks occupy the left side of the graph while the AML marks are still scattered at the right side of the graph. The small number of blue marks is caused by an insufficiency in AML image database, thus further research is still encouraged.

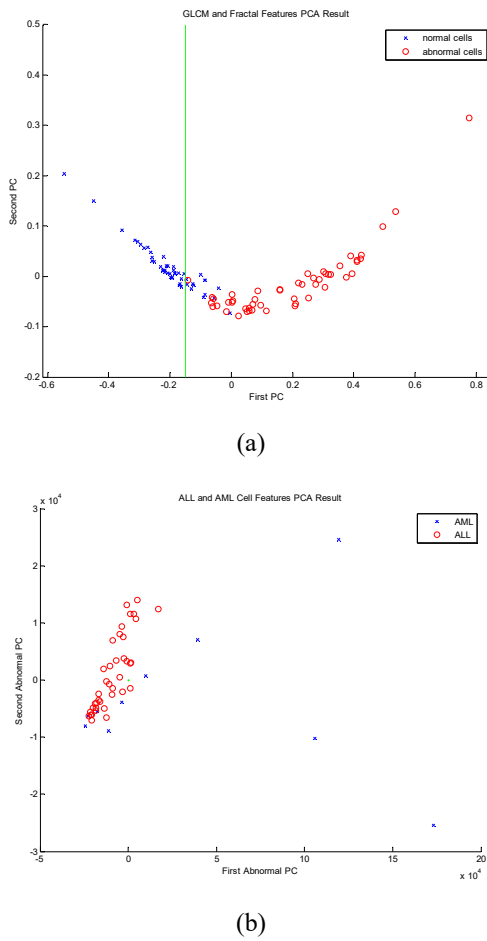


Fig. 8. (a) First PCA result, (b) second PCA result.

4.3 Neural network classification result

The first neural network verification phase classification result is shown in Fig. 9(a) while validation phase classification result is shown in Fig. 9(b). The verification procedure is done by applying the same input training image database to the trained network while validation procedure is done by applying previously unknown image database to the trained network. The verification performance reaches 97.7% accuracy rate

which outperformed Madukhar et al. [4] method with only 93.5% accuracy rate.

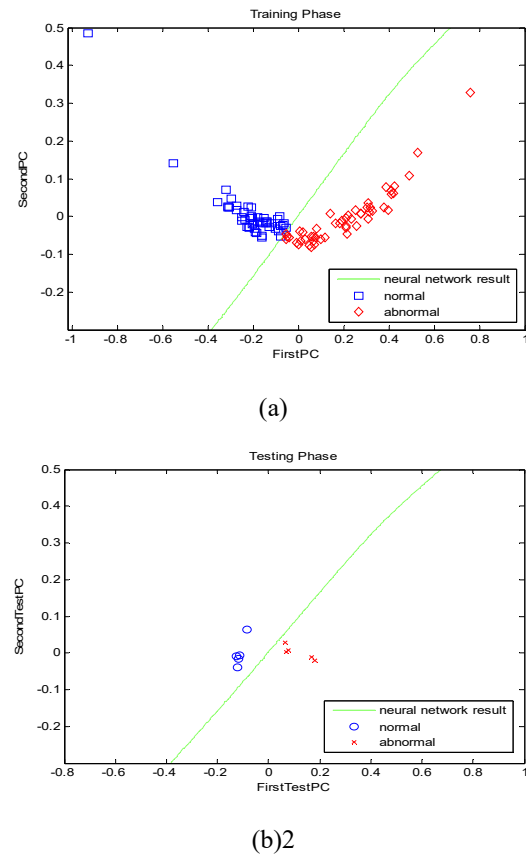


Fig. 9. (a) Verification result, (b) Validation result.

Table 1 Neural network classifier result.

Parameter	Verification performance	Validation performance
	Value	Value
True Positive (TP)	40	5
False Positive (FP)	1	0
True Negative (TN)	48	5
False Negative (FN)	1	0
Specificity (TPR)	97.6%	100 %
Sensitivity (SPC)	98%	100 %
Accuracy	97.7%	100 %

5. Conclusion

The proposed method has been performed on 100 complete blood smear images. 90 images are used for training image while 10 images are kept as validation images. In this experiment, GLCM and fractal features are extracted from an image database to discriminate between normal and abnormal cell images while 5 geometrical features from only the abnormal cell images are extracted in order to discriminate between AML and ALL leukemia type. The sequential neural network classification

performance reaches 97.7% accuracy rate and outperformed our referred publication with only 93.5% accuracy rate. These experiment results are expected to be considered as one of the constructing modules for an automatic leukemia diagnostic decision support system, yet further research is still encouraged in order to acquire a proper classification result between AML and ALL leukemia type.

Acknowledgments

This research was supported by Basic Science Research Program through the National Research Foundation of Korea (NRF) funded by the Ministry of Science and ICT (No. 2016R1D1A3B03931003, No. 2017R1A2B2012456) and MSIP (Ministry of Science and ICT), Korea, under the Grand Information Technology Research Center support program (IITP-2017-2016-0-00318) supervised by the IITP(Institute for Information & communications Technology Promotion)".

References

- [1] V. F. R.D.Labati, "ALL-IDB: The Acute Lymphoblastic Leukemia Image Database for Image Processing," *18th IEEE International Conference on Image Processing*, 2011.
- [2] H. A. R.Soltanzadeh, "Extraction of Nucleolus Candidate Zone in White Blood Cells of Peripheral Blood Smear Images Using Curvelet Transform," *Hindawi Publishing Corporation, Computational and Mathematical Methods in Medicine*, vol. 2012, p. 12, February 2012.
- [3] M. A. N. H. N.H. Harun, "Automated Classification of Blast in Acute Leukemia Blood Samples using HMLP Network," *Proceedings of the 3rd International Conference on Computing and Informatics*, pp. 55-60, June 2011.
- [4] S. A. C. M.Madhukar, "New Decision Support Tool for Acute Lymphoblastic Leukemia Classification," *Proceeding of SPIE-IS&T Electronic Imaging, SPIE*, vol. 8295, 2012.
- [5] E. Berner, "Clinical Decision Support Systems: State of the Art," *Agency for Healthcare Research and Quality Publication*, June 2009.
- [6] D. S. K. A.Z. Chitade, "Color Based Image Segmentation Using K-Means Clustering," *International Journal of Engineering Science and Technology*, vol. 2, pp. 5319-5325, 2010.
- [7] L. C.D.Ruberto, "White Blood Cells Identification and Counting from Microscopic Blood Image," *World Academy of Science, Engineering and Technology*, vol. 73, 2013.
- [8] B. S. S. K. S. L. K. K. I.Vincent, "Feature Selection Using Principal Component Analysis for Leukemia Classification,"

Proceeding of the 10th International Conference on Multimedia Information Technology and Applications 2014, pp. 206-207, July 2014.



Ivan Vincent received the B.S. degree in electrical engineering from Institute Teknologi Bandung, Indonesia, in 2012 and received a master degree in IT Convergence and Application Engineering in Pukyong National University, Korea, in 2015.



Tran Thi Phuong Thanh received the B.S. degree in Information Technology from Water Resources University, Vietnam, in 2015. She is currently studying a master course in IT Convergence and Application Engineering in Pukyong National University, Korea.



Suk-Hwan Lee received a B.S., a M.S., and a Ph. D. Degrees in Electrical Engineering from Kyungpook National University, Korea in 1999, 2001, and 2004 respectively. He is currently an associate professor in Department of Information Security at Tongmyong University. His research interests include multimedia security, digital image processing, and computer graphics.



Ki-Ryong Kwon received the B.S., M.S., and Ph. D. degrees in electronics engineering from Kyungpook National University in 1986, 1990, and 1994 respectively. He worked at Hyundai Motor Company from 1986-1988 and at Pusan University of Foreign Language from 1996-2006. He is currently a professor in Dept. of IT Convergence & Application Engineering at the Pukyong National University. He has researched University of Minnesota in USA on 2000-2002 with Post-Doc, and Colorado State University on 2011-2012 with visiting professor. He was the General President of Korea Multimedia Society on 2015-2016, also was a director of IEEE R10 Changwon section on 2012-2016. His research interests are in the area of digital image processing, multimedia security and watermarking, bioinformatics, weather radar information processing.